Geomechanics and Engineering, *Vol. 18, No. 3 (2019) 299-313*
DOI: https://doi.org/10.12989/gae.2019.18.3.299

One-dimensional nonlinear consolidation behavior of structured soft clay under time-dependent loading

Weizheng Liu[1a], Zhiguo Shi[1b], Junhui Zhang*[2] and Dingwen Zhang[3c]

[1]*School of Civil Engineering, Central South University, Changsha, China*
[2]*National Engineering Laboratory of Highway Maintenance Technology, Changsha University of Science & Technology, Changsha, China*
[3]*School of Transportation, Southeast University, Nanjing, China*

(Received July 21, 2018, Revised June 4, 2019, Accepted June 6, 2019)

Abstract. This research investigated the nonlinear compressibility, permeability, the yielding due to structural degradation and their effects on consolidation behavior of structured soft soils. Based on oedometer and hydraulic conductivity test results of natural and reconstituted soft clays, linear log (1+e) ~ log σ'$_v$ and log (1+e) ~ log k$_v$ relationships were developed to capture the variations in compressibility and permeability, and the yield stress ratio (YSR) was introduced to characterize the soil structure of natural soft clay. Semi-analytical solutions for one-dimensional consolidation of soft clay under time-dependent loading incorporating the effects of soil nonlinearity and soil structure were proposed. The semi-analytical solutions were verified against field measurements of a well-documented test embankment and they can give better accuracy in prediction of excess pore pressure compared to the predictions using the existing analytical solutions. Additionally, parametric studies were conducted to analyze the effects of YSR, compression index (λ_r and λ_c), and permeability index (η_k) on the consolidation behavior of structured soft clays. The magnitude of the difference between degree of consolidation based on excess pore pressure (U_p) and that based on strain (U_s) depends on YSR. The parameter λ_c/η_k plays a significant role in predicting consolidation behavior.

Keywords: nonlinear consolidation; soil structure; semi-analytical solutions; time-dependent loading

1. Introduction

Natural soft clays are generally structured with interparticle bonding developed during depositional and post-depositional processes (Leroueil and Vaughan 1990, Cotecchia and Chandler 2000), and time-dependent external loadings are usually applied during consolidation process (Conte and Troncone 2007, Razouki and Schanz 2011, Liu and Griffiths 2015, Xu *et al.* 2017). The soil structure brings about a significant influence on the compression behavior (Burland 1990, Liu *et al.* 2003, Borja and Choo 2016, Zhang *et al.* 2016). Small compressibility is observed in pre-yield stage due to resistance of soil structure, whereas large compressibility occurs when the effective stress is beyond the consolidation yield stress. The soil permeability is also greatly related to the soil structure and significantly decreases as the structure is damaged (Tavenas *et al*. 1983, Zeng *et al*. 2011, Ozelim *et al.* 2014). Therefore, it is essential when predicting settlement of natural soft soils to use a consolidation model that takes both the nonlinear variations of compressibility, permeability and soil structural characteristics into account.

To investigate the effect of soil structure on one-dimensional consolidation behavior of structured soils, using simply segmented k_v-σ'_v and m_v-σ'_v models incorporating the consolidation yield stress as the segmentation point, Chen *et al*. (2004) and Xie *et al*. (2016) obtained the approximate solution for structured soils under time-dependent loading by transforming structured soils into double-layered soils with the gradually changing thickness of the upper and lower layers, and Hu *et al*. (2017) studied the consolidation behavior of layered structured soils with groundwater drawdown in a confined aquifer using analytical methods, but the nonlinearity of soil were ignored in these studies. Based on the $e \sim \log \sigma'_v$ and $e \sim \log k_v$ linear responses, Rujikiatkamjorn and Indraratna (2015) derived analytical solution for radial consolidation considering soil structure characteristics. However, several researchers pointed out that for structured natural clays with high sensitivity, the compression curve was nonlinear in the $e \sim \log \sigma'_v$ plot due to progressive destructuration, and the compression index along the post-yield stress range was variable (Butterfield 1979, Burland 1990, Chai *et al*. 2004). The nonlinear phenomenon was also observed in $e \sim \log k_v$ relationship of structured soils with high initial void ratio (Mesri and Olson 1971, Zeng *et al*. 2011). Therefore, prediction of consolidation settlement using the linear $e \sim \log \sigma'_v$ and $e \sim \log k_v$ relations may deviate from the actual response.

∗Corresponding author, Professor
E-mail: zjhseu@csust.edu.cn
[a]Associate Professor
E-mail: liuwz2011@csu.edu.cn
[b]Graduate Student
E-mail: 1328092728@qq.com
[c]Professor
E-mail: zhangdw@seu.edu.cn

ISSN: 2005-307X (Print), 2092-6219 (Online)

The objective of this paper is to present one-dimensional nonlinear consolidation solutions of structured soft soils, which are capable of considering the effects of variable compressibility and permeability as well as soil structure. Based on observations from a series of oedometer tests and hydraulic conductivity tests on natural and reconstituted soft clays, the more linear log (1+e) ~ log σ'_v and log (1+e) ~ log k_v relationships were developed and employed to derive the consolidation governing equations. The semi-analytical method was adopted to solve the governing equations of the nonlinear consolidation under time-dependent loading, and the corresponding computer program was also presented. Subsequently, the semi-analytical solutions were validated by the existing analytical solutions in special cases and the results of field tests. Then a parametric study was performed to examine the effects of yield stress ratio, compression index and permeability index on the consolidation behavior of structured soils.

2. Compressibility and permeability evaluation considering soil structure characteristics

2.1 Materials and method

The tested samples were obtained from the Taihu lacustrine-swamp clayey deposit in southeast China. A representative stratigraphic profile of the sampling site is shown in Fig. 1. The relatively homogenous silty clay sublayer was used in this study and undisturbed Taihu clay samples at depths ranging from 3.0 m to 16.0 m were retrieved using the fixed piston thin-walled sampler. Fig. 1 shows some physical properties of the tested samples. The silt is dominant in the soil particle composition and the silt content reachs as high as 70%, and the clay content ranges from 10% to 30%. The magnitude of plasticity index (I_p) varies in a range of 10.2-17.8. Notably, the natural moisture content (w_0) is mostly exceeding the liquid limit (w_L), and the initial void ratio is generally larger than 1.0. The high magnitude of w_0/w_L identifies Taihu clay as a strongly structured soil

The undisturbed oedometer specimens were carefully trimmed directly into the 61.8 mm confining stainless steel ring by applying some downward pressure on the ring to the required height of 20 mm, while the undisturbed hydraulic conductivity specimens were trimmed by hand to nominal diameter of 61.8 mm and height of 40 mm. For preparing the corresponding reconstituted specimens, the trimmings were collected and thoroughly mixed at a water content equal to w_L. Then the samples were consolidated in cylindrical plastic tubes until they reached a suitable consistency and the required void ratio approximately equal to initial void ratio (e_0) of the intact samples.

One-dimensional compression tests were carried out using the standard oedometer apparatus. The consolidation stresses of 12.5 kPa, 25 kPa, 50 kPa, 100 kPa, 200 kPa, 300 kPa, 400 kPa, 800 kPa, 1600 kPa, and 3200 kPa were incrementally applied, and the duration of every load increment is about 24 h.

The falling head hydraulic conductivity tests were performed on undisturbed and remolded specimens during compression to measure the variation of hydraulic conductivity with the void ratio under increasing effective vertical stresses. In the same way as described by Zeng *et al.* (2011), the specimen was mounted into the modified oedometer cell underwater, and then subjected to an increased load at a load incremental ratio of 1.0 (12.5 kPa, 25 kPa, 50 kPa, 100 kPa, 200 kPa, 300 kPa, 400 kPa, 800 kPa and 1600 kPa). When consolidation was completed, the hydraulic conductivity was measured at initial water head of 1.0 m when the applied vertical stress smaller than 200 kPa and 2.0 m when the stress larger than 200 kPa. The duration of the consolidation and hydraulic conductivity test was 3 days for each stage.

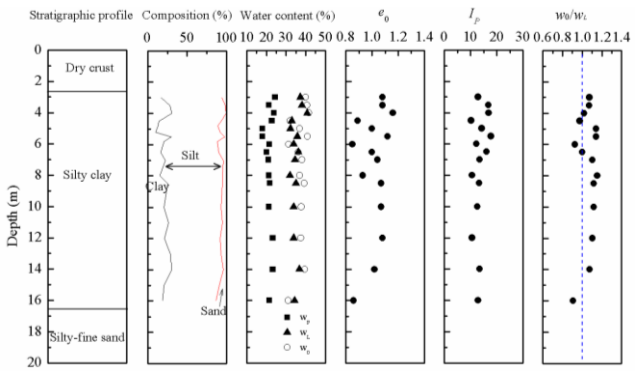

Fig. 1 Geotechnical index properties of Taihu clay

2.2 Test results and analysis

2.2.1 Void ratio-stress relationship

Compression curves for natural typical Taihu clay samples with initial void ratio of 1.16 and 0.84 are plotted in Fig.2 in terms of e versus log σ'_v and log (1+e) versus log σ'_v, respectively. It can be seen that the compression curves in the e - log σ'_v plot are nonlinear due to progressive destructuration when compression stress exceeds the yielding stress. When adopting specific volume v=(1+e) to plot log (1+e) versus log σ'_v, the nonlinear curves in e - log σ'_v plot are made close to linear. This is because of taking the logarithm of the specific volume (1+e) means reducing the distance between the larger e values and increasing the distance between the smaller e values. Fig. 2 also shows results for a wide range of initial void ratio from 1.59 to13.8 of different natural soils in the existing literatures, an inverse "S" shape of the e - log σ'_v compression curves is observed in Fig. 2(a) and the linearity is improved in all cases in Fig. 2(b) which relates log (1+e) to log σ'_v. The similar characteristic was observed by Chai *et al.* (2004) and showed that for natural clays with a sensitivity value greater than 4 the compression curves in the ln(e+e_c) - ln(σ'_v) plot have much better linearity than those in the e - ln(σ'_v) plot, where the value of e_c is varied between –1 and 1. Hence, the e - log σ'_v compression curves with an inverse "S" shape could be well represented by two straight lines in the plot of log (1+e) against log σ'_v, which are divided by the consolidation yield stress.

It has been well known that the compression behaviour of reconstituted clays is controlled by the liquid limit

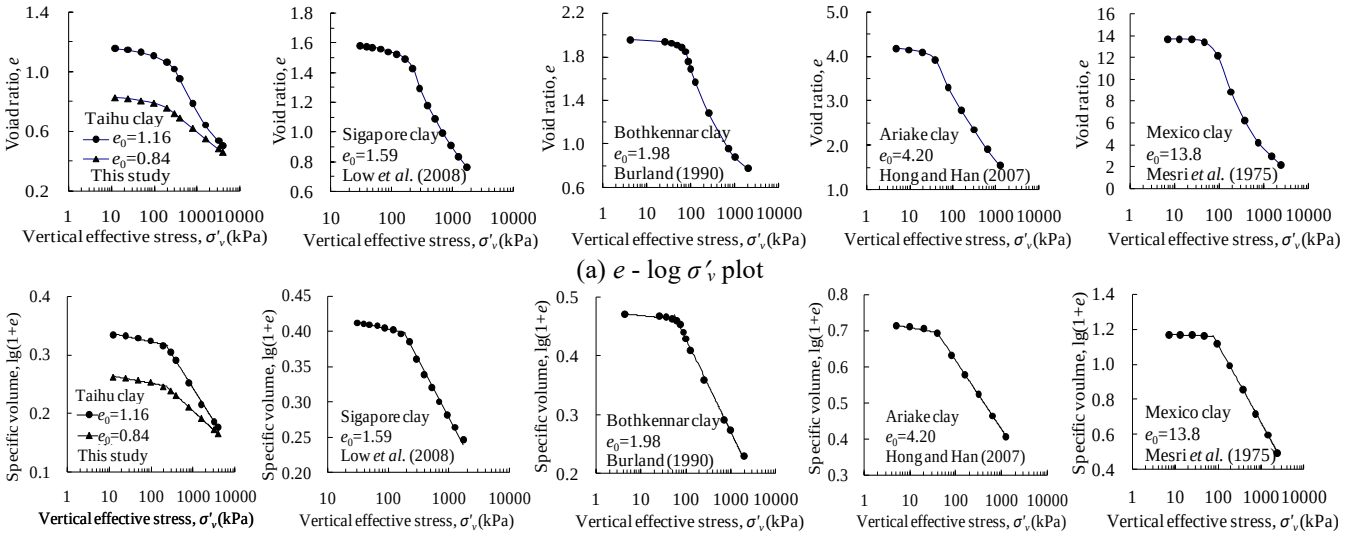

(a) e - log σ'_v plot

(b) log (1+e) - log σ'_v plot

Fig. 2 Compression curves of five natural sedimentary clays in two different patterns

Table 1 Reconstituted clays with different liquid limits

Soils	Depth h (m)	Liquid limit w_L (%)	Plastic limit w_P (%)	Source of data
Taihu clay	4.0	40.8	23.9	This study
Taihu clay	5.0	32.3	18.0	This study
Lower Cromer Till	-	25.0	-	Burland (1990)
London Clay	-	67.5	-	Burland (1990)
Argile Plastique	-	128.0	-	Burland (1990)
Bothkennar clay	13.7	77.0	31.0	Nash *et al.* (1992)
Bothkennar clay	5.2	85.0	37.0	Nash *et al.* (1992)
Ariake clay	2-12	98.3	37.4	Hong *et al.* (2004)
Ariake clay	2-12	112.5	45.1	Hong *et al.* (2004)
Ariake clay	2-12	140.1	45.8	Hong *et al.* (2004)

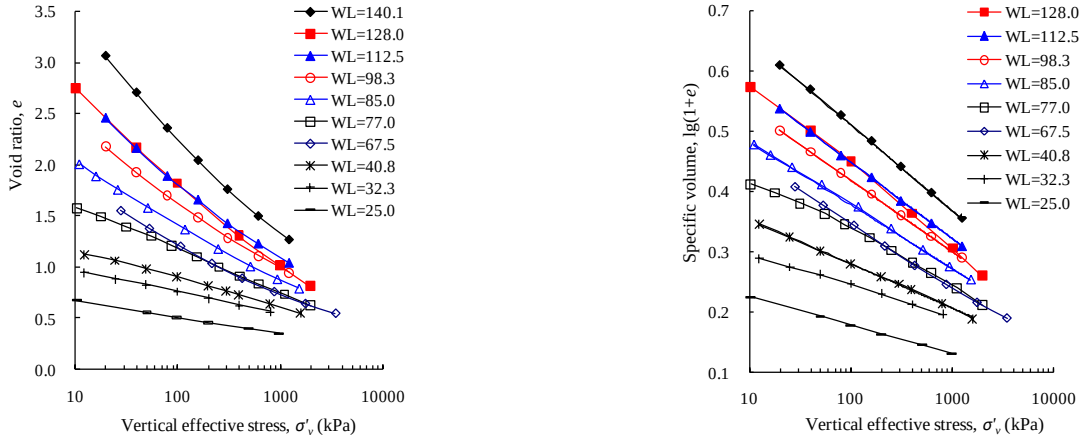

(a) e - log σ'_v plot

(b) log (1+e) - log σ'_v plot

Fig. 3 Compression curves of different reconstituted soils in two different patterns

(Skempton 1970, Burland 1990). The one-dimensional compression curves for some reconstituted clays covering a wide range of liquid limits listed in Table 1 are shown in Fig. 3. It is evident from Fig. 3(a) that the e - log σ'_v compression curves are all similar in shape being slightly concave upwards and not completely linear. The compression test data in Fig. 3(a) are replotted in terms of log (1+e) versus log σ'_v, as shown in Fig. 3(b). It can be seen that the bilogarithmic plot would not change the well-established linearity of compression curves, and all the data

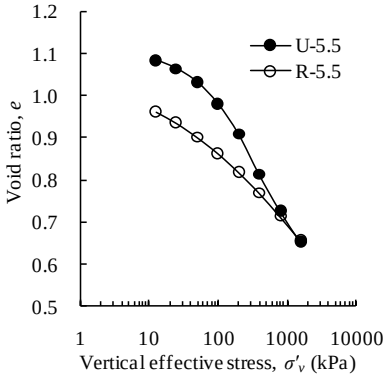

(a) e - log σ'_v relationship

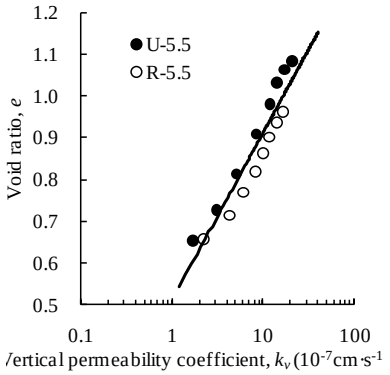

(b) Corresponding e - log k_v relationship

Fig. 4 Compressibility and permeability behavior of Taihu clay in undisturbed and remolded states

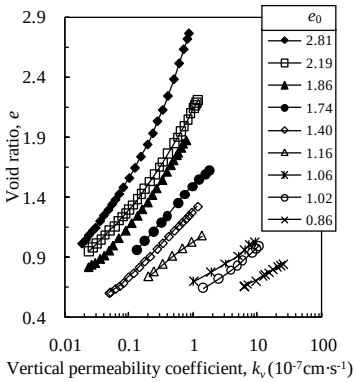

(a) e - log σ'_v plot

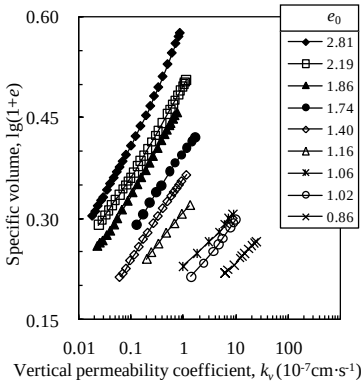

(b) e - log k_v plot

Fig. 5 Permeation curves of different clays in two different patterns

Table 2 Sources of different clays with a wide range of initial void ratios

Soils	Depth, h (m)	e_0	e_L	Source of data
Taihu clay	4.2	0.86	0.88	This study
Taihu clay	6.0	1.02	0.92	This study
Taihu clay	8.8	1.06	0.99	This study
St-Hilaire	9.5	1.86	1.49	Tavenas *et al.* (1983)
St-Thuribe	6.9	1.40	1.19	Tavenas *et al.* (1983)
Backcebol	5.4	2.19	2.00	Tavenas *et al.* (1983)
Lilla Mellosa	4.3	2.81	3.00	Tavenas *et al.* (1983)
Berthierville clay	4.0	1.74	1.32	Leroueil *et al.* (1988)
Bothkennar clay	1.2	1.16	1.33	Nash *et al.* (1992)

with different liquid limits can be represented by different straight lines. Therefore, the more linear log (1+e) - log σ'_v relation is used in this paper to interpret the compression test data for both natural and reconstituted soils.

2.2.2 Void ratio–permeability relationship

The permeability is an independent and important parameter for consolidation analysis of clay foundations. Fig. 4 shows the compressibility and permeability of Taihu clay at a depth 5.5 m in undisturbed and remolded states. It can be seen that the shape of e - log k_v permeation curves behave differently from that of e - log σ'_v compression curves of the undisturbed specimens. The compression behaviour of natural clays can be classified into pre-yield state with small deformation and post-yield with large deformation, which differs from that of remolded clays, while the e - log k_v relationship of undisturbed specimen is almost identical to that of the remolded specimen. The permeability of the clay in undisturbed and remolded states is identical under the same void ratio. This leads to the conclusion that the soil structure, exactly the interparticle bonding, does not significantly influence the change mode of permeability with void ratio. This finding is consistent with the results presented by Lapierre *et al.* (1990), Horpibulsuk *et al.* (2007), and Zeng *et al.* (2011).

Since the coefficient of permeability varies with void ratio (fabric), irrespective of the soil structure (interparticle bonding), Fig. 5 presents some different permeation curves of clays covering a wide range of initial void ratios listed in Table 2. The permeation curve of soil with higher initial void ratio lies above that of soil with lower initial void ratio. The higher initial void ratio, the more nonlinear relationship and more concave shape of the e - log k_v curve are observed. Tavenas *et al.* (1983) showed that the linear relationship of e - log k_v was valid for strains < 20% and initial void ratios < 2.5, and Horpibulsuk *et al.* (2007) also reported the nonlinear relationship of the e - log k_v of Bangkok clays with void ratios varying from 0.2 to about 1.0 times the initial void ratios. Thus, similar to the compression test data, the form of log (1+e) - log k_v was used to interpret the data of permeability coefficient. As can be seen from Fig. 5, the permeation curves in the log (1+e) -

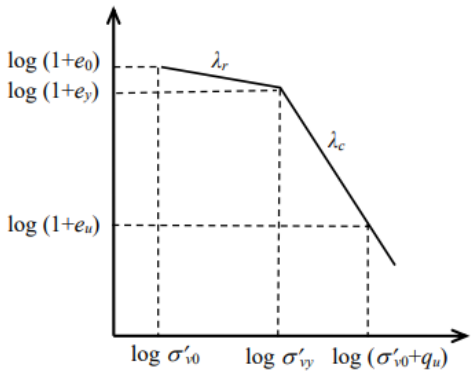

(a) log (1+e) - log σ'_v compression model

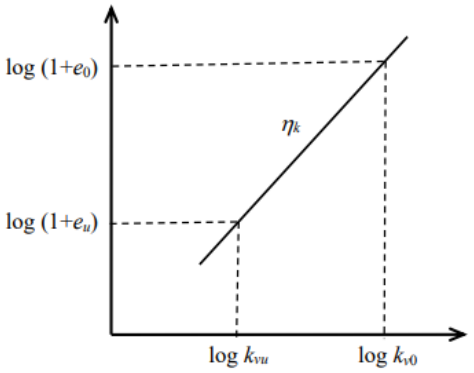

(b) log (1+e) - log k_v permeability model

Fig.6 Constitutive relationships of structured soils

log k_v plot have much better linearity than those in the e – log k_v plot. Hence, the relationship between void ratio and permeability coefficient could be expressed well by a straight line in the log (1+e) - log k_v plot within the full range of strains during compression for both natural and reconstituted soils.

2.2.3 Bilinear compression and permeability relationships

As illustrated in the previous sections, the bilogarithmic method can be used to represent well the compressibility and permeability behavior. The compression curve of natural structured clays can be expressed by two straight lines, and the stress at the intersection point of the two straight lines is the consolidation yield stress. The permeation curve can be expressed by a straight line in the plot log (1+e) against log k_v. With reference to Fig. 6, the compressibility relationships in the whole compression zone are described by

$$\log(1+e)=\log(1+e_0)-\lambda_r\log(\sigma'_v/\sigma'_{v0}) \qquad \sigma'_v\le\sigma'_{vy} \quad (1a)$$

$$\log(1+e)=\log(1+e_0)-\lambda_r\log(YSR)-\lambda_c\log(\sigma'_v/\sigma'_{vy}) \qquad \sigma'_v>\sigma'_{vy} \quad (1b)$$

Void ratio - permeability relationship is given by

$$\log(1+e)=\log(1+e_0)+\eta_k\lg(k_v/k_{v0}) \qquad (2)$$

where, YSR is the yielding stress ratio and given by $YSR=\sigma'_{vy}/\sigma'_{v0}$; k_v and k_{v0} are coefficients of permeability corresponding to e and e_0; λ_r and λ_c are the compression index of pre-yield and post-yield states in the log (1+e) - log σ'_v plot, respectively; and η_k is the permeability index in the log (1+e) - log k_v plot.

3. Nonlinear consolidation model incorporating effect of soil structure

3.1 Equations and solutions

The current analysis deals with one-dimensional nonlinear consolidation of a finite thickness natural structured soil layer under time-dependent loading. Fig. 7 is the schematic diagram, where H is the thickness of the soil layer with a pervious upper boundary and an impervious lower boundary. Compared with classical Terzaghi's theory, the non-linear material properties expressed in Eqs. (1) and (2) are assumed to be incorporated in this analysis, and the imposed loading $q(t)$, distributing uniformly on the top of the soil surface, changes with time. Other assumptions are the same as those in Terzaghi's theory.

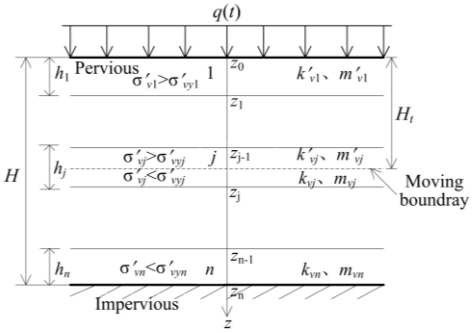

Fig. 7 Schematic diagram for one-dimensional consolidation of structured soil foundation

During the consolidation process, if the effective stress σ'_v is greater than the consolidation yield stress σ'_{vy}, the soil structure of upper layer will be destroyed firstly and its compression index will change from λ_r in pre-yield state to λ_c in post-yield state, but the compressibility and permeability of lower layer soil will be the same as those of the natural structured soil in pre-yield state. The soil structure of the upper subsoil gradually damages downwards with the dissipation of pore pressure, and hence the interface of destructured zone and structured zone is defined as moving boundary, the depth of moving boundary is H_t. It can be known that H_t increases from 0 to H with development of consolidation. If $\sigma'_v<\sigma'_{vy}$, the breakdown of soil structure will not occur and the permeability coefficient and compression index are kept same as those of the pre-yield state.

3.1.1 Governing equations

Based on Eqs. (1) and (2)

$$\begin{cases} m_v=-\dfrac{1}{1+e_0}\dfrac{\partial e}{\partial\sigma'_v}=m_{v0}\left(\dfrac{\sigma'_{v0}}{\sigma'_v}\right)^{\lambda_r+1} & \sigma'_v\le\sigma'_{vy} \\ m'_v=-\dfrac{1}{1+e_0}\dfrac{\partial e}{\partial\sigma'_v}=m_{v0}\dfrac{\lambda_c}{\lambda_r}\left(\dfrac{1}{YSR}\right)^{\lambda_r+1}\left(\dfrac{\sigma'_{vy}}{\sigma'_v}\right)^{\lambda_c+1} & \sigma'_v>\sigma'_{vy} \end{cases} \qquad (3)$$

$$\begin{cases} k_v = k_{v0}\left(\dfrac{\sigma'_{v0}}{\sigma'_v}\right)^{\frac{\lambda_r}{\eta_k}} & \sigma'_v \le \sigma'_{vy} \\ k'_v = k_{v0}\left(\dfrac{1}{YSR}\right)^{\frac{\lambda_r}{\eta_k}}\left(\dfrac{\sigma'_{vy}}{\sigma'_v}\right)^{\frac{\lambda_c}{\eta_k}} & \sigma'_v > \sigma'_{vy} \end{cases} \tag{4}$$

where m_v and k_v are the coefficients of volume compressibility and permeability in pre-yield state, respectively; m'_v and k'_v are the coefficients of volume compressibility and permeability in post-yield state, respectively; m_{v0}= initial coefficient of compressibility given by $m_{v0}=\lambda_r/\sigma'_{v0}$.

The continuity equation for one-dimensional consolidation is

$$\frac{\partial q}{\partial z} = \frac{1}{1+e_0}\frac{\partial e}{\partial t} \tag{5}$$

where q is the flow per unit area and given by $q=\dfrac{k_v}{\gamma_w}\dfrac{\partial u}{\partial z}$, u is the excess water pressure; γ_w is the unit weight of water.

According to Terzaghi's principle of effective stress, σ'_v can be expressed as

$$\sigma'_v = \sigma'_{v0} + q(t) - u \tag{6a}$$

Hence,

$$\frac{\partial \sigma'_v}{\partial t} = \frac{\partial q(t)}{\partial t} - \frac{\partial u}{\partial t} \tag{6b}$$

Substituting Eqs. (3), (4) and (6b) into Eq.(5), the governing equations for one-dimensional consolidation of natural structured soil layer can be given by

$$\begin{cases} c_{v0}\left(\dfrac{\sigma'_{v0}}{\sigma'_v}\right)^{\frac{\lambda_r}{\eta_k}-\lambda_r-1}\dfrac{\partial^2 u}{\partial z^2} = \dfrac{\partial u}{\partial t} - \dfrac{\partial q(t)}{\partial t} & H_t \le z \le H \\ c_{v0}\dfrac{\lambda_r}{\lambda_c}\left(\dfrac{1}{YSR}\right)^{\frac{\lambda_r}{\eta_k}-\lambda_r-1}\left(\dfrac{\sigma'_{vy}}{\sigma'_v}\right)^{\frac{\lambda_c}{\eta_k}-\lambda_c-1}\dfrac{\partial^2 u}{\partial z^2} = \dfrac{\partial u}{\partial t} - \dfrac{\partial q(t)}{\partial t} & 0 \le z < H_t \end{cases} \tag{7}$$

where c_{v0} is the initial coefficient of consolidation and given by

$$c_{v0} = \frac{k_{v0}}{m_{v0}\gamma_w} = \frac{k_{v0}\sigma'_{v0}}{\lambda_r\gamma_w} \tag{8}$$

The initial and boundary conditions of the problem can be simplified as follows

$$z = 0:\ u = 0 \tag{9a}$$

$$z = H:\ \frac{\partial u}{\partial z} = 0 \tag{9b}$$

$$t = 0:\ u = q(t)\big|_{t=0} \tag{9c}$$

When $\lambda_r=\lambda_c$ and $\lambda_c/\eta_k = \lambda_c + 1$, the coefficient of consolidation keeps constant with time and Eq. (7) can be analytically solved. Apart from the special condition, Eq. (7) is non-linear partial differential equation and does not have an analytical solution with the boundary conditions mentioned above.

3.1.2 Semi-analytical solutions

As indicated above, the moving boundary surface H_t varies with consolidation time t, and soil layers above and below H_t have different compressibility. Due to the complexity involved, a general analytical solution to Eq. (7) is difficult to obtain. Based on the discretization of time and space, a semi-analytical method is used to solve Eq.(7) and analyze the nonlinear consolidation behavior of structured soils.

According to Xie and Pan's semi-analytical method, the soil stratum is divided into n thin layers of equal thickness h_j (h_j =H/n) and the consolidation time is divided into m small time steps (Zhang *et al*. 2015). The coordinate z has its origin at the top surface, as seen in Fig.7, denoting the distance between the origin and the bottom of each layer as z_i. Thus, z_0=0, z_i=iH/n, i=1, 2, 3, …, n, and z_n=H.

Corresponding to the discretization of time, the load increment at an arbitrary step k is given by

$$\Delta q_k = q_k - q_{k-1} = q(t_k) - q(t_{k-1}) \tag{10}$$

For the ramp loading occurred usually in engineering practice, the load increment Δq_k can be expressed as

$$\Delta q_k = \begin{cases} \dfrac{q_u}{t_c}(t_k - t_{k-1}) & 0 \le t_k \le t_c \\ 0 & t_k > t_c \end{cases} \tag{11}$$

where q_u is ultimate load and t_c defines the end of the loading stage.

When the time interval is small enough, both the coefficients of compressibility and permeability at each thin layer as well as the imposed loading in each small time step can be assumed to be constant. Thus, the problem of one-dimensional consolidation of structured soil with varied compressibility and permeability under time-dependent loading has been reduced to the problem of one-dimensional linear consolidation of layered soils. To obtain the approximate solution, the coefficients of compressibility and permeability of layer j at the time t_{k-1} are used to calculate the coefficient of consolidation at the time t_k (k>1). Besides, the effective overburden stress (σ'_{v0}) and consolidation yield stress (σ'_{vy}) of the soil stratum are assumed to distribute uniformly with depth. Hence, the average coefficient of consolidation for layer j (j=1, 2, 3, …, n) at the time t_k is given by

$$c_{vjk} = \begin{cases} c_{v0j}\left(\dfrac{\sigma'_{v0}}{\sigma'_{vj(k-1)}}\right)^{\frac{\lambda_r}{\eta_k}-\lambda_r-1} & \sigma'_{vj(k-1)} \le \sigma'_{vy} \\ c_{v0j}\dfrac{C'_{rj}}{C'_{cj}}\left(\dfrac{1}{YSR}\right)^{\frac{\lambda_r}{\eta_k}-\lambda_r-1}\left(\dfrac{\sigma'_{vy}}{\sigma'_{vj(k-1)}}\right)^{\frac{\lambda_c}{\eta_k}-\lambda_r-1} & \sigma'_{vj(k-1)} > \sigma'_{vy} \end{cases} \tag{12}$$

where $\sigma'_{vj(k-1)}$ is the average effective stress of layer j at the time t_{k-1} and can be expressed as

$$\sigma'_{vj(k-1)} = \sigma'_{v0} + q(t_{k-1}) - \bar{u}_{j(k-1)} \tag{13}$$

where $\sigma'_{v0} = \gamma' H/2$; $\bar{u}_{j(k-1)}$ is the average excess pore

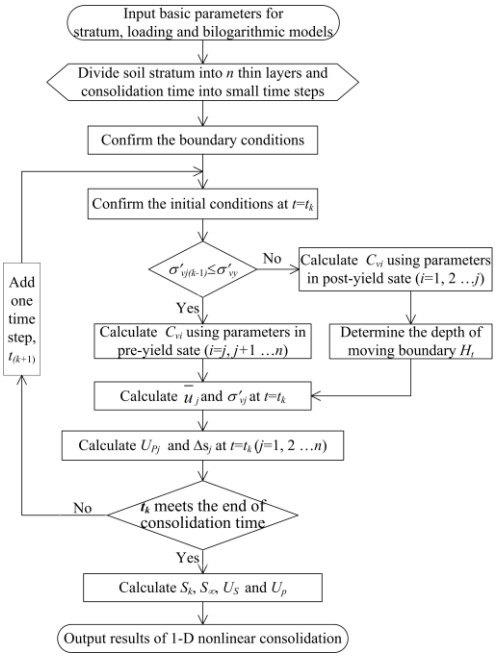

Fig. 8 Calculation procedure

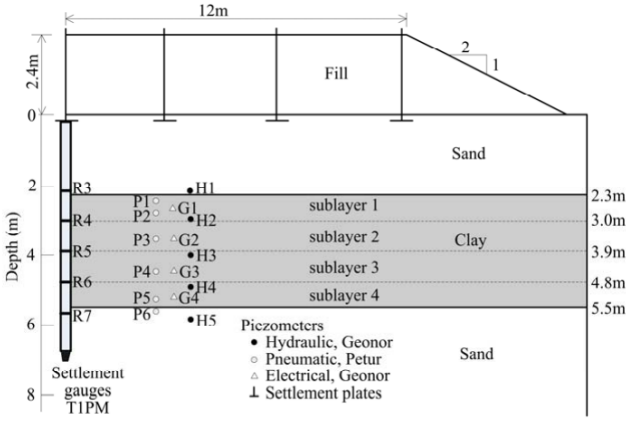

Fig. 9 Layout of the instrumentation at Berthierville (from Kabbaj *et al.* 1988)

water pressure of layer j at the time t_{k-1} and can be obtained as

$$\bar{u}_{j(k-1)} = \frac{1}{h_j}\int_{z_{j-1}}^{z_j} u_j(z, t_{k-1})dz \tag{14}$$

Thus, the governing equation for an arbitrary layer j at an arbitrary step k can be written as

$$c_{vjk}\frac{\partial^2 u_{jk}}{\partial z^2} = \frac{\partial u_{jk}}{\partial t}, \quad j = 1, 2, \text{L}\ , n. \tag{15}$$

The one-dimensional nonlinear consolidation of structured soils at an arbitrary step k has been translated into one-dimensional consolidation of layered soils under constant loading. Correspondingly, the initial and boundary condition for Eq. (15) becomes

$$u_{jk} = \bar{u}_{j(k-1)} + q_k - q_{k-1} \tag{16a}$$

$$z = z_j:\ u_j = u_{j+1};\ k_{vj}\frac{\partial u_j}{\partial z} = k_{v(j+1)}\frac{\partial u_{j+1}}{\partial z} \tag{16b}$$

$$z = 0:\ u_1 = 0 \tag{16c}$$

$$z = H:\ \frac{\partial u_n}{\partial z}\Big|_{z=H} = 0 \tag{16d}$$

The excess pore water pressure of layer j at $t=t_k$, i.e., u_{jk} in Eq. (15), can be obtained by Xie and Pan's semi-analytical method (see Appendix). And the corresponding value $\bar{u}_{jk}$ can also be obtained using Eq. (14).

The compression of layer j at $t=t_k$ can then be given as

$$s_j = \int_{z_{j-1}}^{z_j}\varepsilon_{jk}dz \approx \begin{cases}[1-(\dfrac{\sigma'_{v0}}{q(t_k)+\sigma'_{v0}-\bar{u}_{jk}})^{\lambda_r}]h_j & \sigma'_{vjk} \le \sigma'_{vy} \\ [1-(\dfrac{1}{YSR})^{\lambda_r}(\dfrac{\sigma'_{vy}}{q(t_k)+\sigma'_{v0}-\bar{u}_{jk}})^{\lambda_c}]h_j & \sigma'_{vjk} > \sigma'_{vy}\end{cases} \tag{17}$$

When the structure damage surface occurs in the ith layer, and the depth of moving boundary surface is H_t ($z_{i-1}< H_t <z_i$), the compression of the whole soil stratum at $t=t_k$ then can be given by

$$\begin{aligned} S_k = \sum_{j=1}^{n} s_j = \sum_{j=1}^{i-1}[1-(\frac{1}{YSR})^{\lambda_r}(A_{jk})^{\lambda_c}]h_j + \sum_{j=i+1}^{n}[1-(A_{jk})^{\lambda_r}]h_j + \\ [1-(\frac{1}{YSR})^{\lambda_r}(B_{ik})^{\lambda_c}](H_t - z_{i-1}) + [1-(B_{ik})^{\lambda_r}](z_i - H_t)\end{aligned} \tag{18}$$

where $A_{jk} = \dfrac{\sigma'_{vy}}{q(t_k)+\sigma'_{v0}-\bar{u}_{jk}};\ B_{ik} = \dfrac{\sigma'_{vy}}{q(t_k)+\sigma'_{v0}-\bar{u}_{ik}}$.

At the end of consolidation (i.e., $t\to\infty$), $\bar{u}_{jk}=0$, $H_t=H$, hence the ultimate settlement can be given by

$$S_\infty = [1-(\frac{1}{YSR})^{\lambda_r}(\frac{\sigma'_{vy}}{q_u+\sigma'_{v0}})^{\lambda_c}]H \tag{19}$$

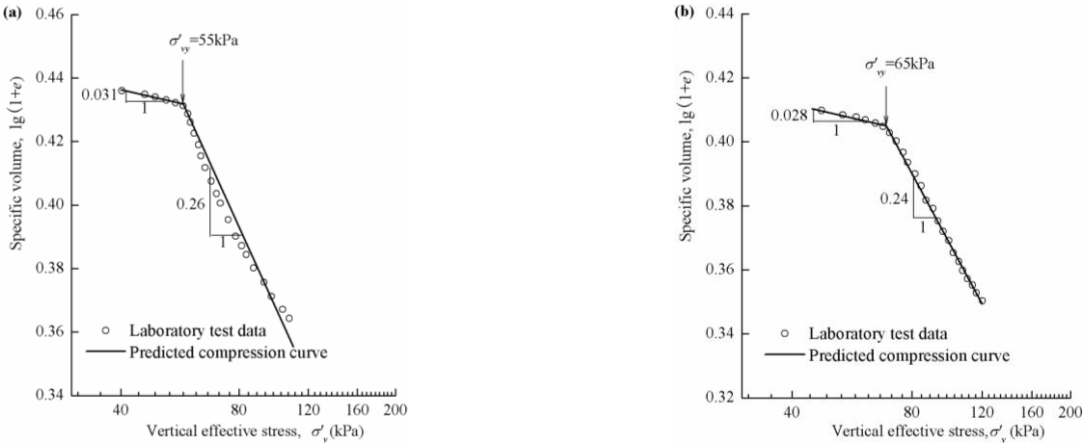

(a) Sublayer 2 (3.0 m-3.9 m) (b) Sublayer 3 (3.9 m-4.8 m)

Fig. 10 Bilogarithmic compression curves of undisturbed Bertbierville clays (interpreted from Kabbaj *et al.*1988)

Table 3 Soil parameters for Berthierville clay embankment

Soils	Depth (m)	e_0	λ_r	λ_c	η_k	k_{v0} (10^{-7}cm·s^{-1})	σ'_{v0} (kPa)	σ'_{vy} (kPa)	q_u (kPa)
Sublayers 1-2	2.3~3.9	1.73	0.031	0.26	0.134	2.80	40	55	44
Sublayers 3-4	3.9~5.5	1.55	0.028	0.24	0.127	4.50	50	65	44

The average degree of consolidation of the whole soil stratum defined in terms of settlement can then be obtained as

$$U_S=\frac{S_k}{S_\infty}=\frac{\sum_{j=1}^{i-1}[1-(\frac{1}{YSR})^{\lambda_r}(A_{jk})^{\lambda_c}]h_j+\sum_{j=i+1}^{n}[1-(A_{jk})^{\lambda_r}]h_j+[1-(\frac{1}{YSR})^{\lambda_r}(B_{ik})^{\lambda_c}](H_t-z_{i-1})+[1-(B_{ik})^{\lambda_r}](z_i-H_t)}{[1-(\frac{1}{YSR})^{\lambda_r}(\frac{\sigma'_{vy}}{q_u+\sigma'_{v0}})^{\lambda_c}]H} \quad (20)$$

where $\rho_j=h_j/H$; $U_{pj}(t_k)=[q(t_k)-\bar{u}_{jk}]/q_u$, the average degree of consolidation of layer j defined in terms of excess pore water pressure.

In Terzaghi's 1-D consolidation theory, the average degree of consolidation defined in terms of settlement is the same as that defined in terms of pore water pressure, namely, $U_p=U_s$. However, when the influence of soil structure and nonlinearity are taken into consideration, it can be seen from Eqs. (20) and (21) that U_p is different from U_s .

In order to investigate the nonlinear consolidation behavior of structured soil, a computer code was developed by c++ programming based on the semi-analytical solutions illustrated above, and the flow chart of this program can be seen from Fig. 8.

3.2 Comparison and verification

A well-instrumented case presented originally by Kabbaj *et al.* (1988) is used to examine the validity of the semi-analytical method by comparing the measured results with the computed values obtained from the presented procedure. The case concerns a test embankment constructed on a soil deposit consisting of a soft grey silty

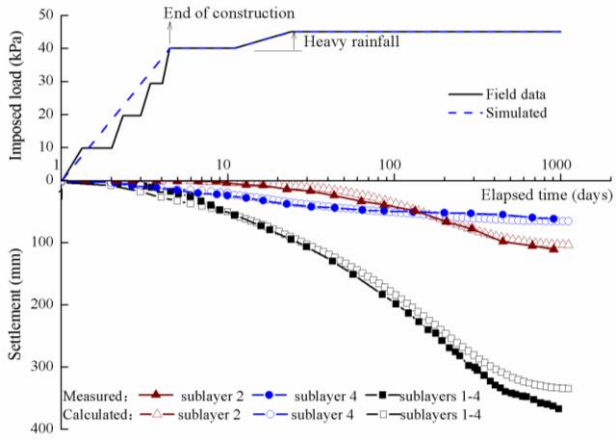

Fig. 11 Comparisons of measured and simulated settlements for different sublayers

clay layer sandwiched between an upper layer of sand and a lower layer of sand at Berthierville site (Fig. 9), which is located on the north shore of the St Laurent River between Quebec City and Montreal (Kabbaj *et al.* 1988). The clay layer, which is of interest in this study, is 3.2 m thick and lies at a depth of 2.3 m from the ground surface. The plasticity index decreases with depth from 27 to 16, and the water content is constant and equal to 62% in the upper half of the layer and then decreases linearly to 47% at the bottom of the clay layer. The test embankment is circular with a diameter of 24 m at the crest, and has a height of 2.4 m and a slope of 1 vertical to 2 horizontal. With such soil profile and lateral width of the embankment compared to the thickness of the clay layer, the case is certainly close to one-dimensional consolidation under double-drainage condition.

As shown in Fig. 9, a series of instrumentation was installed at various depths for monitoring the pore water pressure and settlement occurring during and after the construction. It consisted of 15 piezometers, of which 12 in the clay layer, one in the upper sand layer, and two in the lower sand layer. The instrumentation also included deep settlement gauges at initial depths of 2.1, 3.0, 3.9, 4.8, and 5.7 m, thus dividing the clay layer into four sublayers: sublayer 1 between depths 2.3 and 3.0 m, sublayer 2

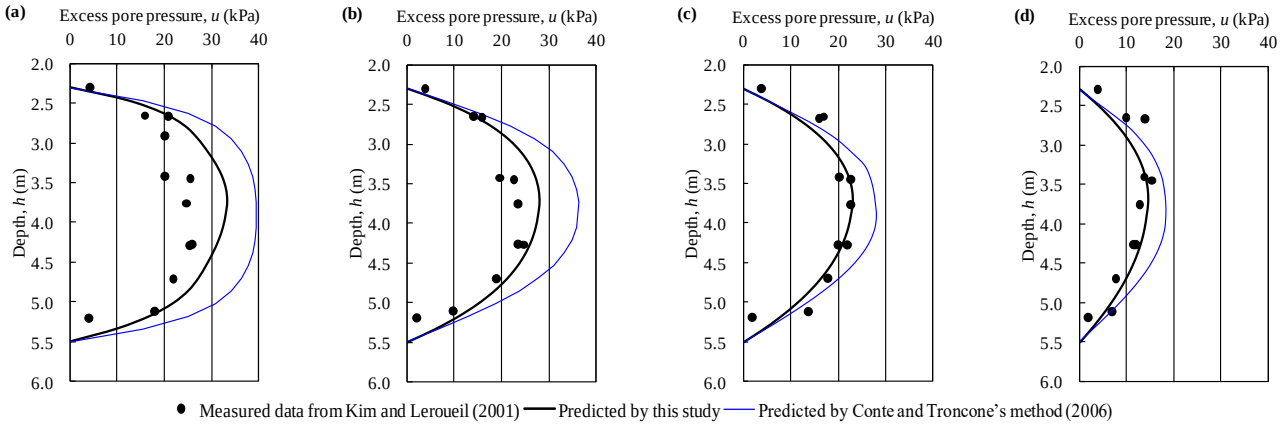

(a) After 10 days (b) After 50 days (c) After 100 days (d) After 200 days

Fig. 12 Comparisons of measured excess pore pressure with predictions from this study and Conte and Troncone (2006) at different times after construction

between depths 3.0 and 3.9 m, sublayer 3 between depths 3.9 and 4.8 m, and sublayer 4 between depths 4.8 and 5.5 m. Based on the index properties presented by Kabbaj *et al.* (1988), the behavior of sublayer 1 is similar to that of sublayer 2, and the behavior of sublayer 3 is similar to that of sublayer 4, thus the same parameters are adopted for sublayers 1 and 2 and sublayers 3 and 4 in this study, respectively.

As stated previously, except for conventional parameters such as e_0 and k_{v0}, four new parameters related to the soil nonlinearity and soil structure are introduced in the developed consolidation model, i.e., λ_r, λ_c, η_k, and *YSR*. Fig. 10 shows the bilogarithmic compression curves interpreted from the conventional oedometer tests (MSL_{24}) performed by Kabbaj *et al*. (1988) on the specimens taken in the middle of sublayer 2 and sublayer 3. Obviously, the laboratory compression test data can be fitted well by two straight lines. The compression index λ_r and λ_c can be obtained from the slopes of the straight lines in pre-yield and post-yield state, respectively. And the consolidation yield stress σ'_{vy} can be determined from the stress related to the intersection point of the two straight lines, then *YSR* is equal to the ratio of σ'_{vy} to σ'_{v0}. The permeability index used in this calculation can be calculated from the empirical relationship $\eta_k = 0.044e_0 + 0.007e_0/e_L + 0.049$ proposed by Liu (2011) based on enough hydraulic test results, where e_L represents the void ratio at the liquid limit and can be obtained from Kabbaj *et al*. (1988). The calculation parameters for the nonlinear consolidation of the entire clay layers are listed in Table 3, and the values of e_0, k_{v0}, and σ'_{v0} are obtained from the research done by Kim and Leroueil (2001).

The embankment loading is simulated by two-stage linear loading process. As shown in Fig. 11, during stage 1 the embankment construction was complete in 4 days, and the loading was increased to 39 kPa. Following a rest period of one week, an additional loading as a result of heavy rain was applied during stage 2, therefore the maximum intensity of imposed loading q_u reached to 44 kPa after 24 days. Fig. 11 presents the calculated and measured settlements under the time-dependent loading for sublayer 2 and 4 as well as for the entire clay layer (sublayer 1 to 4). At the early stage of consolidation, the agreement between calculated and measured settlements is satisfactory. As the consolidation time increases, the proposed method gives slight underestimation of the magnitude of settlement compared to the measured result of the entire clay layer. This could be due to the neglection of soil creep in the current model, which greatly influences consolidation deformation characteristics of clays, especially for the structured soft clays at latter stage of consolidation.

Another comparison of calculated and measured results is presented in Fig. 12 in terms of excess pore pressure versus depth at different times after construction. The calculations are carried out using the presented nonlinear semi-analytical solutions and the linear analytical solutions proposed by Conte and Troncone (2006). Due to the fact that the decrease in permeability is proportional to the decrease in compressibility during the consolidation process, and the assumption that c_v remains constant in the Conte and Troncone method, the constant values of m_v and k_v are adopted, where m_v is assumed to be determined by $m_v = \lambda_c/\sigma'_{v0}$, and k_v is approximatively equal to k_{v0}. The calculations using the presented solutions generally give satisfactory agreement with the measured results, except for the case of after 10 days, which overpredicts the excess pore pressure due to the simulated loading is larger than the actual applied loading at this stage. However, the predictions using Conte and Troncone's solutions give higher excess pore pressure compared with the measured results and calculations from the presented method. This is because the effect of soil structure is not considered in this prediction, which results in a smaller coefficient of consolidation compared with the actual condition. It is noted that the discrepancy between the predictions using nonlinear solutions and linear solutions decreases with the increase of consolidation time. This is the reason that the effective stress increases as the dissipation of excess pore pressure, and the structural collapse occurs gradually, which leads to the decrease in coefficient of consolidation.

All of the comparisons between calculated and measured results show that the proposed semi-analytical solutions have good predictive ability on one-dimensional

nonlinear consolidation of structured soft clay under time-dependent loading. As can be observed in Figs. 11 and 12, the proposed method predicts the performance of the natural soils more accurately than the existing analytical solutions by considering the effects of soil nonlinearity and soil structure.

3.3 Parametric study

In this section, the effects of soil nonlinearity and soil structure on the consolidation behavior were firstly examined, and then several simulations were performed to study the influences of the different values of *YSR*, λ_r/λ_c, λ_c/η_k, and the loading rate on the consolidation behavior of structured soft soils. For the parametric analysis, the soil is under the case of linear loading, in which the ultimate load q_u is 100 kPa and the time of achieving the ultimate load, t_c, is 500 days. Relevant parameters used in the analysis are given in Table 4. Fig. 13 shows normalized excess pore pressure with depth ratio using different solutions at time factor T_v=0.15, where $T_v=c_{v0}t/H^2$, in which $c_{v0}=k_{v0}$ $_{v0}/(\lambda_c\gamma_w)$. As can be noted, the calculations for the linear consolidation using the constant coefficients of compressibility and permeability, that is to say the coefficient of consolidation is kept constant as c_{v0}, differ significantly from these obtained using the nonlinear solutions. The excess pore pressure calculated from the linear solution is larger than that calculated from the nonlinear solution with soil structure taking into account when *YSR*=1.5, whereas is smaller than that calculated from the nonlinear solution without considering soil structure when *YSR*=1.0 and $\lambda_r=\lambda_c$=0.12. It can be seen that from the degree of consolidation with time factor T_v using different solutions as shown in Fig. 14, the linear solution gives an underestimation for both the settlement rate and excess pore pressure dissipation rate compared to the nonlinear solution with *YSR*=1.5, while overestimates both the settlement rate and excess pore pressure dissipation rate compared to the nonlinear solution with *YSR*=1.0. Moreover, it should be stated that there is no difference between the degree of consolidation based on excess pore pressure (U_p) and the degree of consolidation based on strain (U_s) in linear consolidation, however, for nonlinear consolidation U_p is different from U_s. For the case of *YSR*=1.5, U_p is larger than U_s at the early stage of consolidation, while U_p is less than U_s when *YSR*=1.0.

3.3.1 Effect of YSR on the consolidation behavior

As illustrated previously, the *YSR* can represent the degree of soil structure of natural soil. The *YSR* = 1.2, 15, 1.8 and 2.1 were chosen for the analysis to examine the effect of soil structure on the consolidation behavior. All other parameters are the kept the same as those in Table 3. Fig. 15 shows the degree of consolidation with time factor T_v for different values of *YSR*. It is observed that both U_p and U_s increase with the increasing of *YSR*, and the increased amplitude of U_p is greater than that of U_s. This demonstrates the consolidation progress of strongly structured clays is much faster. At the early stage of consolidation, the dissipation of excess pore water pressure is quicker than the development of settlement due to the structure resistance when the effective stress is less than consolidation yield stress, which results in small deformation and high coefficient of consolidation. At the later stage of consolidation, U_s is greater due to the collapse of soil structure when the effective stress is beyond consolidation yield stress, which results in large amount deformation and small coefficient of consolidation. The

Table 4 Parameters used in the parametric analysis

λ_r	λ_c	η_k	k_{v0} (10^{-7}cm·s^{-1})	e_0	σ'_{v0} (kPa)	q_u (kPa)	*YSR*	H (m)
0.015	0.12	0.10	4.0	1.08	50	100	1.5	10

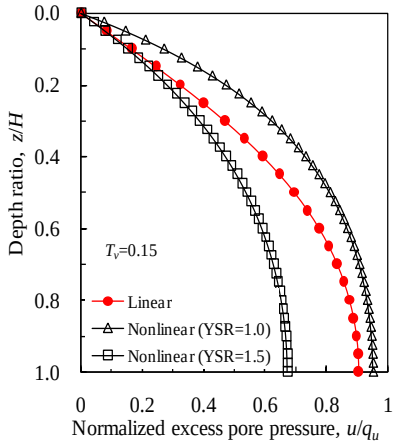

Fig. 13 Normalized excess pore pressure with depth ratio using different solutions

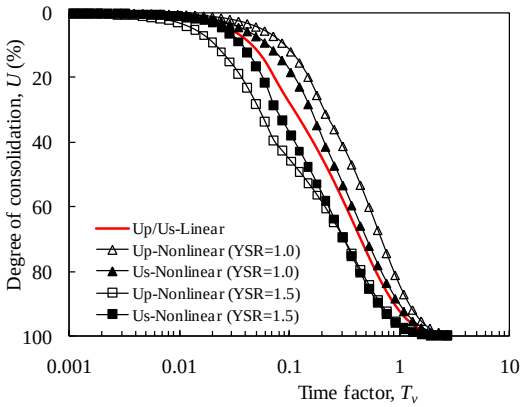

Fig. 14 Degree of consolidation with time factor using different solutions

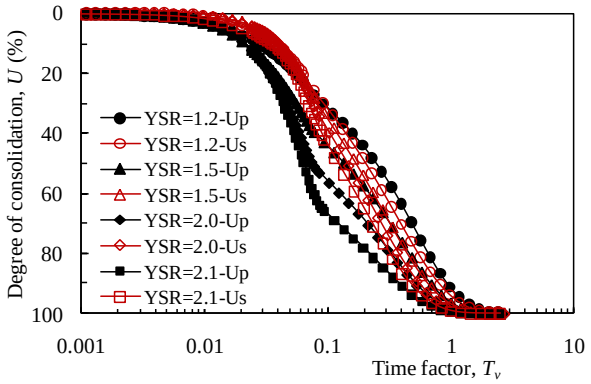

Fig. 15 Effect of *YSR* on degree of consolidation

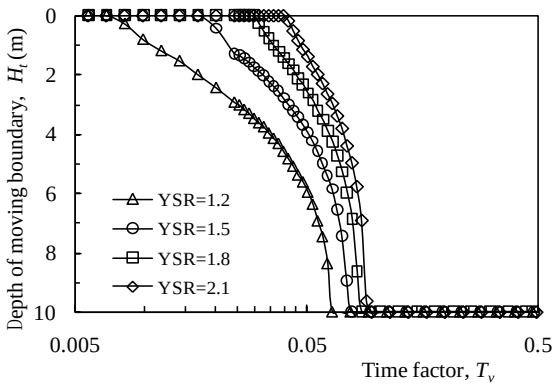

Fig. 16 Effect of *YSR* on the depth of moving boundary

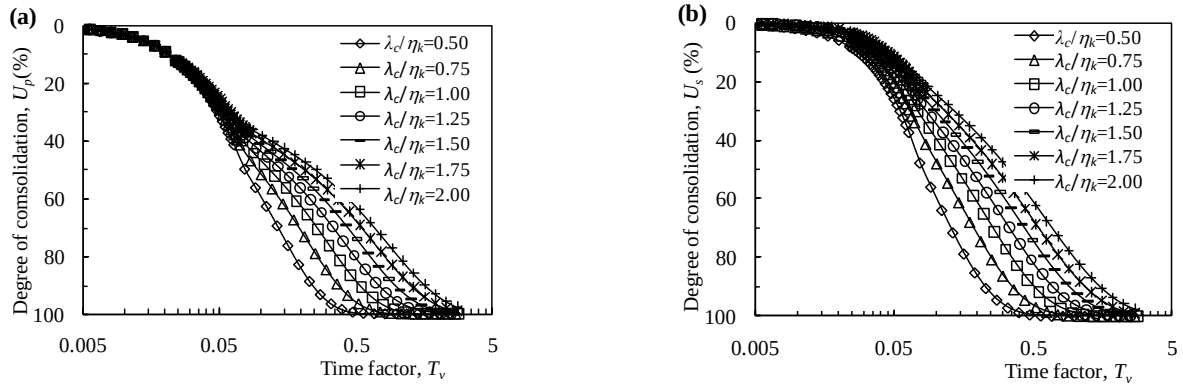

(a) U_p versus T_v (b) U_s versus T_v

Fig. 17 Effect of λ_c/η_k on degree of consolidation

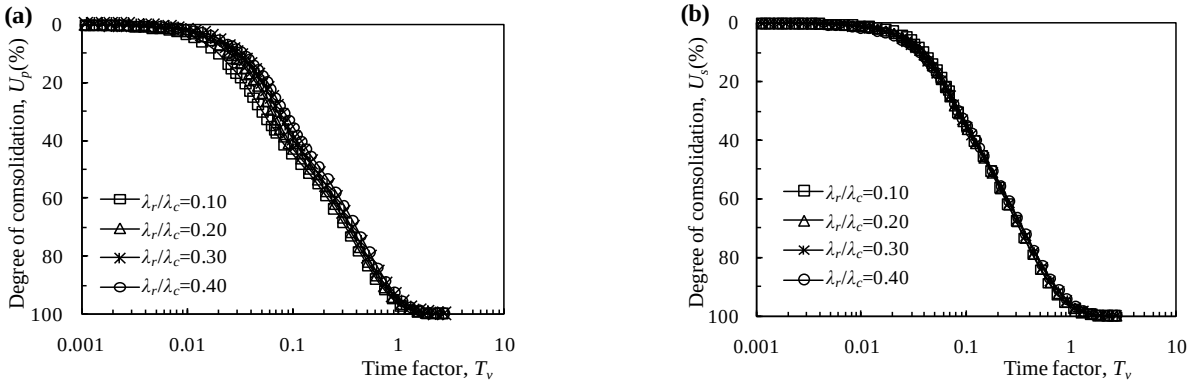

(a) U_p versus T_v (b) U_s versus T_v

Fig. 18 Effect of λ_r/λ_c on degree of consolidation

magnitude of the difference between U_p and U_s depends on the value of *YSR*, and the higher *YSR*, the larger difference is observed.

Fig. 16 shows the variation of moving boundary surface with time factor T_v for different values of *YSR*. It can be seen that at the same T_v the depth of moving boundary decreases with the increasing of *YSR*. The structure of soil gradually destroys downwards with the dissipation of the pore pressure, and a smaller *YSR* results in earlier damage of the soil structure.

3.3.2 Effect of λ_c/η_k on the consolidation behavior

Liu (2011) has reported that in bilogarithmic plot the typical value of λ_r generally ranges from 0.003 to 0.05, λ_c generally ranges from 0.066 to 0.221, and η_k generally ranges from 0.077 to 0.173 for natural soft soils. In order to study the effect of λ_c/η_k on consolidation behavior, λ_c values are changed to 0.05, 0.075, 0.10, 0.125, 0.15 and 0.20, respectively. By keeping η_k = 0.10, these changes result in λ_c/η_k equal to 0.50, 0.75, 1.00, 1.25, 1.50, 1.75 and 2.00, respectively. Other parameters are kept the same as in Table 3. Fig. 17 shows the degree of consolidation with time factor T_v for different values of λ_c/η_k. It is observed that soil consolidates more quickly as λ_c/η_k decreases and the effect appears to be more pronounced when λ_c/η_k is less than 1.0. Moreover, it can be seen from Eqs. (3) and (4) that the value of λ_c/η_k controls both m_v and k_v. Larger λ_c/η_k results in

smaller soil module, and thus the consolidate process of soil layers is much slower. This demonstrates that the stiffer and more permeable soils, the higher rate of excess pore pressure dissipation and settlement development.

3.3.3 Effect of λ_r/λ_c on the consolidation behavior

In order to study the effect of λ_r/λ_c on consolidation behavior, λ_c is kept constant as 0.12 and λ_r is changed to 0.012, 0.024, 0.036, and 0.048, respectively. Thus λ_r/λ_c is equal to 0.1, 0.2, 0.3, and 0.4, respectively. The other parameters are kept the same as in Table 3. Fig.18 shows the degree of consolidation with time factor T_v for different values of λ_r/λ_c. It can be seen that the rate of excess pore pressure dissipation increases with decreasing of λ_r/λ_c at the early stage of consolidation. However at the later stage of consolidation, the curves U_p versus T_v of different λ_r/λ_c gradually converge towards the same consolidation curve. The main reason is that the compressibility index for this case is kept the same as 0.12 after the collapse of structure. Moreover, the variation of λ_r/λ_c has little impact on the rate of settlement development. The curves U_s versus T_v of different λ_r/λ_c are almost identical in the whole consolidation process.

4. Conclusions

The semi-analytical solutions for one dimensional consolidation of soft clay under time-dependent loading incorporating the effects of soil nonlinearity and soil structure were proposed. The solutions were verified against field measurement of a well-documented embankment constructed on structured soft soil. Parametric studies were then conducted to examine the effects of compression index, permeability index, yield stress ratio and loading rate on the consolidation behavior. From the results of this study, the following conclusions can be drawn:

• Bilinear log $(1+e)$ - log σ'_v model with the break in behavior controlled by the consolidation yield stress was developed to capture the variation in compressibility.

• The soil structure (interparticle bonding) has no effect on the mode of changing in the permeability coefficient with void ratio. The linear log $(1+e)$ - log k_v model was developed to capture the variation in permeability.

• Incorporating the log $(1+e)$ - log σ'_v and log $(1+e)$ - log k_v relationships, the governing equations for one-dimensional nonlinear consolidation under time-dependent loading were derived, and were solved by adopting the semi-analytical method.

• Four parameters related to the soil nonlinearity (λ_r, λ_c, and η_k) and structural characteristics (YSR) are introduced in the semi-analytical solutions, the proposed solutions can reduce to the existing linear analytical solutions in particular case.

• The prediction of excess pore-water pressure using the proposed nonlinear solutions provided a better agreement with the field measurement compared to the predictions using the linear solutions with constant coefficient of consolidation.

• For nonlinear consolidation, the degree of consolidation based on excess pore pressure (U_p) is different from the degree of consolidation based on strain (U_s). The magnitude of the difference between U_p and U_s depends on the value of YSR, and the higher YSR, the larger difference appears.

• Both U_p and U_s increase with decrease of λ_c/η_k, and this effect appears to be more pronounced when λ_c/η_k is less than 1.0. With decreasing of λ_r/λ_c, U_p increases at the early stage of consolidation, whereas U_s has no significant change. The λ_c/η_k plays a significant role in predicting the consolidation rate.

Acknowledgments

This study was supported by the National Natural Science Foundation of China (51208517), Hunan Provincial Natural Science Foundation of China (2019JJ40344), and the Fundamental Research Funds for the Central Universities of Central South University (2019zzts620). The authors are grateful to Dr. Ruikun Zhang at Southeast University and Mr. Yu Zhao for their help in the oedometer tests and hydraulic conductivity tests.

References

Borja, R.I. and Choo, J. (2016), "Cam-Clay plasticity, Part VIII: A constitutive framework for porous materials with evolving internal structure", *Comput. Meth. Appl. Mech. Eng.*, **309**, 653-679. https://doi.org/10.1016/j.cma.2016.06.016.

Burland, J.B. (1990), "On the compressibility and shear strength of natural clays", *Geotechnique*, **40**(3), 329-378. https://doi.org/10.1680/geot.1990.40.3.329.

Butterfield, R. (1979), "A natural compression law for soils", *Geotechnique*, **29**(4), 469-480.

Chai, J.C., Miura, N., Zhu, H.H. and Yudhbir (2004), "Compression and consolidation characteristics of structured natural clay", *Can. Geotech. J.*, **41**(6), 1250-1258. https://doi.org/10.1139/t04-056.

Chen, Y.M., Tang, X.W. and Wang, J. (2004), "An analytical solution of one dimensional consolidation for soft sensitive soil ground", *Int. J. Numer. Anal. Meth. Geomech.*, **28**(9), 919-930. https://doi.org/10.1002/nag.353.

Conte, E. and Troncone, A. (2007), "Nonlinear consolidation of thin layers subjected to time-dependent loading", *Can. Geotech. J.*, **44**(6), 717-725. https://doi.org/10.1139/t07-015.

Cotecchia, F. and Chandler, R.J. (2000), "A general framework for the mechanical behaviour of clays", *Geotechnique*, **50**(4), 431-447.

Hong, Z.S., Negami, T. and Guo, H.L. (2004), "Gravitational sedimentation behavior of sensitive marine Ariake clays", *Mar. Georesour. Geotechnol.*, **22**(1-2), 49-63. https://doi.org/10.1080/10641190490467765.

Hong, Z.S. and Han, J. (2007), "Evaluation of sample quality of sensitive clay using intrinsic compression concept", *J. Geotech. Geoenviron. Eng.*, **133**(1), 83-90. https://doi.org/10.1061/(ASCE)1090-0241(2007)133:1(83).

Horpibulsuk, S., Shibuya, S., Fuenkajorn, K. and Katkan, W. (2007), "Assessment of engineering properties of Bangkok clay", *Can. Geotech. J.*, **44**(2), 173-187. https://doi.org/10.1139/t06-101.

Hu, A.F., Xia, C.Q., Wu, H., Xie, K.H. and Yan, L.H. (2017), "A study on one-dimensional consolidation of layered structured aquitard soils in a leakage system", *Mar. Georesour. Geotechnol.*, **35**(3), 318-329.

https://doi.org/10.1080/1064119X.2016.1164264.
Kabbaj, M., Tavenas, F. and Leroueil, S. (1988), "In situ and laboratory stress-strain relationships", *Geotechnique*, **38**(1), 83-100. https://doi.org/10.1680/geot.1988.38.1.83.
Kim, Y.T. and Leroueil, S. (2001), "Modeling the viscoplastic behaviour of clays during consolidation application to Berthierville clay in both laboratory and field conditions", *Can. Geotech. J.*, **38**(3), 484-497. https://doi.org/10.1139/t00-108.
Lapierre, C., Leroueil, S. and Locat, J. (1990), "Mercury intrusion and permeability of Louiseville clay", *Can. Geotech. J.*, **27**(5), 568-579. https://doi.org/10.1139/t90-090.
Leroueil, S., Diene, M., Tavenas, F., Kabbaj, M. and Rochelle, P.L. (1988), "Direct determination of permeability of clay under embankments", *J. Geotech. Eng.*, **114**(6), 645-657. https://doi.org/10.1061/(ASCE)0733-9410(1988)114:6(645).
Leroueil, S. and Vaughan, P.R. (1990), "The general and congruent effects of structure in natural soils and weak rocks", *Geotechnique*, **40**(3), 467-488. https://doi.org/10.1680/geot.1990.40.3.467.
Liu, J.C. and Griffiths, D.V. (2015), "A general solution for 1D consolidation induced by depth-and time-dependent changes in stress", *Geotechnique*, **65**(1), 66-72. https://doi.org/10.1680/geot.14.P077.
Liu, M.D., Carter, J.P. and Desai C.S. (2003), "Modeling compression behavior of structured geomaterials", *Int. J. Geomech.*, **3**(2), 191-204. https://doi.org/10.1061/(ASCE)1532-3641(2003)3:2(191).
Liu, W.Z. (2011), "In-situ mechanical behavior analysis of saturated clay and engineering application", Ph.D. Dissertation, Southeast University, Nanjing, China.
Low, H.E., Phoon, K.K., Tan, T.S. and Leroueil, S. (2008), "Effect of soil microstructure on the compressibility of natural Singapore marine clay", *Can. Geotech. J.*, **45**(2), 161-176. https://doi.org/10.1139/T07-075.
Mesri, G. and Olson, R.E. (1971), "Mechanisms controlling the permeability of clays", *Clay. Clay Miner.*, **19**(3), 151-158. https://doi.org/10.1346/CCMN.1971.0190303.
Mesri, G., Rokhsar, A. and Bohor, B.F. (1975), "Composition and compressibility of typical samples of Mexico City clay", *Geotechnique*, **25**(3), 527-554. https://doi.org/10.1680/geot.1975.25.3.527.
Nash, D., Sills, G.C. and Davison, L.R. (1992), "One-dimensional consolidation testing of soft clay from Bothkennar", *Geotechnique*, **42**(2), 241-256. https://doi.org/10.1680/geot.1992.42.2.241.
Ozelim, L.C.D.M., de Carvalho, J.C., Cavalcante, A.L.B., da Silva, J.P. and Muneton, C.M.G. (2014), "Novel approach to consolidation theory of structured and collapsible soils", *Int. J. Geomech.*, **15**(4), 1-11. https://doi.org/10.1061/(ASCE)GM.1943-5622.0000409.
Razouki, S.S. and Schanz, T. (2011), "One-dimensional consolidation under haversine repeated loading with rest period", *Acta Geotechnica*, **6**(1), 13-20. https://doi.org/10.1007/s11440-010-0132-1.
Skempton, A.W. (1970), "The consolidation of clays by gravitational compaction", *Quart. J. Geol. Soc.*, **125**(1-4), 373-411. https://doi.org/10.1144/gsjgs.125.1.0373.
Tavenas, F., Leblond, P., Jean, P. and Leroueil, S. (1983), "The permeability of natural soft clays. Part II: Permeability characteristics", *Can. Geotech. J.*, **20**(4), 645-660.
Xie, K.H. and Pan, Q.Y. (1995), "Theory of one-dimensional consolidation of layered soils under variable loading", *Chin. J. Geotech. Eng.*, **17**(5), 80-85.
Xie, K.H., Xia, C.Q., An, R., Hu, A.F. and Zhang, W.P. (2016), "A study on the one-dimensional consolidation of double-layered structured soils", *Comput. Geotech.*, **73**, 189-198. https://doi.org/10.1016/j.compgeo.2015.12.007.
Xu, C.J., Chen, Q.Z., Liang, L.J. and Fan, X.Z. (2017), "Analysis of consolidation of a soil layer with depth-dependent parameters under time-dependent loadings", *Eur. J. Environ. Civ. Eng.*, **6**(sup1), 1-13. https://doi.org/10.1080/19648189.2017.1385539.
Zhang, S., Li, H.C. and Teng, J.D. (2016), "A new constitutive model for structures soil", *Geomech. Eng.*, **11**(5), 725-738. http://dx.doi.org/10.12989/gae.2016.11.5.725.
Zhang, J.H., Cen, G.M., Liu, W.Z. and Wu, H.X. (2015), "One dimensional consolidation of double-layered foundation with depth-dependent initial excess pore pressure and additional stress", *Adv. Mater. Sci. Eng.*, **4**, 1-13. http://dx.doi.org/10.1155/2015/618717.
Zeng, L.L., Hong, Z.S., Cai, Y.Q. and Han, J. (2011), "Change of hydraulic conductivity during compression of undisturbed and remolded clays", *Appl. Clay Sci.*, **51**(1-2), 86-93. https://doi.org/10.1016/j.clay.2010.11.005.

CC

Notation

A_{jk}	constant related to stress of layer j
B_{ik}	constant related to stress of layer including the moving boundary surface
c_v	coefficient of consolidation
c_{v0}	initial coefficient of consolidation, k_{v0} $_{v0}/(\lambda_r\gamma_w)$
e	void ratio
e_0	initial void ratio
e_L	void ratio at the liquid limit
h_j	thickness of each layer of the entire soil
H	thickness of the entire soil layer
H_t	depth of moving boundary
k_v	yield stress ratio
k_{v0}	compression index in pre-yield state
k'_v	compression index in post-yield state
m_v	volume compressibility coefficient in pre-yield state
m_{v0}	initial coefficient of compressibility
m'_v	volume compressibility coefficient in post-yield state
u	excess pore water pressure
u_{jk}	excess pore water pressure of different depths of layer j at $t=t_k$
$\bar{u}_{jk}$	average excess pore water pressure of layer j at $t=t_k$ the time of achieving the ultimate load

U_p consolidation degree based on excess pore pressure

U_s consolidation degree based on strain

q flow per unit area

$q(t)$ time-dependent loading

q_u ultimate imposed load

Δq_k load increment at an arbitrary step k

s_j compression of layer j at $t=t_k$

S_k compression of the whole soil stratum at $t=t_k$

S_∞ ultimate settlement of the whole soil stratum

t consolidation time

t_c construction time

t_k time at an arbitrary step k

T_v time factor

w_0 natural moisture content

w_L liquid limit

w_P plastic limit

YSR yield stress ratio ($\sigma'_{vy}/\sigma'_{v0}$)

z any depth

z_i distance between the origin and bottom of each layer

γ_w unit weight of water

σ'_v vertical effective stress

σ'_{v0} effective overburden stress

σ'_{vy} consolidation yield stress

λ_r compression index in pre-yield state

λ_c compression index in post-yield state

η_k permeability index in the log $(1+e)$ - log k_v plot

Appendix: Detailed derivation of u_{jk}

According to Xie and Pan's method (1995), The dimensionless parameters were defined as follows

$$a_i = \frac{k_{vi}}{k_{v0}},\quad b_i = \frac{m_{vi}}{m_{v0}},\quad \rho_i = \frac{h_j}{H},\quad \mu_i = \sqrt{\frac{b_i}{a_i}}\quad i=1,2,3,\ldots,n. \tag{A1}$$

The corresponding solution of Eq.(15) can be given as

$$u_{jk} = (\bar{u}_{j(k-1)} + q_k - q_{k-1})\sum_{m=1}^{\infty} C_m g_{mi}(z) e^{-\beta_m t}\quad i=1,2,3,\ldots,n. \tag{A2}$$

where

$$g_{mi}(z) = A_{mi}\sin\left(\mu_i\lambda_m\frac{z}{H}\right) + B_{mi}\cos\left(\mu_i\lambda_m\frac{z}{H}\right) \tag{A3}$$

$\beta_m = \frac{c_{v0}\lambda_m^2}{H^2}$, c_{v0} is the initial coefficient of consolidation of soil before the collapse of the structure; and A_{mi} and B_{mi} can be calculated using the following recursive formula

$$\left.\begin{aligned}&\begin{bmatrix}A_{m1} & B_{m1}\end{bmatrix}^T = \begin{bmatrix}1 & 0\end{bmatrix}^T\\ &\begin{bmatrix}A_{m1} & B_{m1}\end{bmatrix}^T = S_i\begin{bmatrix}A_{m(i-1)} & B_{m(i-1)}\end{bmatrix}^T\quad i=2,3,\mathrm{L}\ ,n.\end{aligned}\right\} \tag{A4}$$

where

$$\left.\begin{aligned}&\begin{bmatrix}A_{m1} & B_{m1}\end{bmatrix}^T = \begin{bmatrix}1 & 0\end{bmatrix}^T\\ &\begin{bmatrix}A_{m1} & B_{m1}\end{bmatrix}^T = S_i\begin{bmatrix}A_{m(i-1)} & B_{m(i-1)}\end{bmatrix}^T\quad i=2,3,\mathrm{L}\ ,n.\end{aligned}\right\} \tag{A5}$$

where

$$A_i = \sin\left(\mu_i\lambda_m\frac{z_{i-1}}{H}\right)\quad B_i = \sin\left(\mu_{i-1}\lambda_m\frac{z_{i-1}}{H}\right)\quad C_i = \cos\left(\mu_i\lambda_m\frac{z_{i-1}}{H}\right)\quad D_i = \cos\left(\mu_{i-1}\lambda_m\frac{z_{i-1}}{H}\right)$$

$$d_i = \frac{k_{v(i-1)}}{k_{vi}}\sqrt{\frac{c_{vi}}{c_{v(i-1)}}} = \sqrt{\frac{a_{i-1}b_{i-1}}{a_i b_i}}$$

λ_m is the positive root of the eigen-equation, as follows

$$S_{n+1}\cdot S_n\cdot S_{n-1}\mathrm{L}\ S_2\cdot S_1 = 0 \tag{A6}$$

where

$$S_1 = \begin{bmatrix}1 & 0\end{bmatrix}^T\quad S_{n+1} = \begin{bmatrix}\cos(\mu_n\lambda_m) & -\sin(\mu_n\lambda_m)\end{bmatrix}$$

The coefficient C_m can be obtained as follows

$$C_m = \frac{\sum_{i=1}^{n} b_i\int_{z_{i-1}}^{z_i} g_{mi}(z)\,dz}{\sum_{i=1}^{n} b_i\int_{z_{i-1}}^{z_i} g_{mi}^2(z)\,dz} = \frac{2\sum_{i=2}^{n}\sqrt{a_i b_i}\left[A_{mi}(C_i - D_{i+1}) + B_{mi}(B_{i+1} - A_i)\right]}{\sum_{i=2}^{n}\sqrt{a_i b_i}\left[\mu_i\rho_i\lambda_m\left(A_{mi}^2 + B_{mi}^2\right) + \left(B_{mi}^2 - A_{mi}^2\right)(D_{i+1}B_{i+1} - C_i A_i) + 2A_{mi}B_{mi}\left(C_i^2 - D_{i+1}^2\right)\right]} \tag{A7}$$